Tuning extrinsic noise effects on a small genetic circuit

Mohamed N.M. Bahrudeen[1] and Andre S. Ribeiro[1,2,3]

[1]Laboratory of Biosystem Dynamics, BioMediTech Institute and Faculty of Biomedical Sciences and Engineering, Tampere University of Technology, 33101, Tampere, Finland
[2]CA3 CTS/UNINOVA. Faculdade de Ciencias e Tecnologia, Universidade Nova de Lisboa, Quinta da Torre, 2829-516, Caparica, Portugal.
[3]Multi-scaled biodata analysis and modelling Research Community, Tampere University of Technology, 33101, Tampere, Finland
andre.ribeiro@tut.fi

Abstract

Measurements at the single cell level showed that monoclonal *Escherichia coli* cells differ widely in the numbers of components affecting gene expression dynamics. Using a stochastic model of a 2-genes symmetric toggle switch with realistic multi-step promoter initiation kinetics and empirically validated parameter values, we investigate the role of transcription initiation kinetics on the degree with which cell-to-cell variability in cellular components generates cell-to-cell diversity in switch dynamics. We find that while the mean switching frequency is determined by the promoter kinetics, the cell to cell diversity of this frequency depends both on promoter kinetics and diversity in RNA polymerase numbers. At a microscale level, the main regulator of the cell to cell variability in protein numbers (of both genes in ON and OFF states) is the promoters kinetics, not the diversity in RNA polymerase numbers. We conclude that the promoters kinetics is a critical regulator of the toggle switch dynamics and that can be used as a regulatable filter of extrinsic noise.

Introduction

Escherichia coli executes major behavioral changes by tuning the numbers of the regulatory molecules of the transcriptional and translational machineries, such as RNA polymerase (RNAP) core enzymes, σ factors, and ribosomes (Jishage et al, 1996)(Rahman et al, 2006).

E.g., in the case of σ factors, due to the limited number of RNAP core enzymes (Farewell et al, 1998), as the number of a specific σ factor increases, the number of RNAPs carrying that σ factor increases and, thus, the activity of the promoters associated to that σ factor increases by direct positive regulation, while, the activity of the promoters associated to other σ factors is expected to decrease by indirect negative regulation (Jishage et al, 1996)(Rahman et al, 2006).

Interestingly, the response of genes' activity to these global changes is highly heterogeneous (Farewell et al, 1998). This is due the promoter-dependent selectivity for σ factors (Hengge-Aronis 2002), the action of transcription factors (Farewell et al, 1998) and, in the case of indirect negative regulation, differences in the multi-step kinetics of transcription initiation of the promoters (Kandavalli et al, 2016).

Given this, and making use of stochastic models, we recently hypothesized and showed that the dynamics of the rate-limiting steps in transcription initiation (Lloyd-Price et al, 2006)(McClure, 1980) influences a gene's responsiveness to extrinsic noise (Bahrudeen et al, 2017).

Following this, and given that previous studies have shown that fluctuations in RNA numbers over time can strongly affect the kinetics of small genetic circuits, such as switches and clocks (Arkin et al, 1998)(Ribeiro 2007a)(Ribeiro 2007b), here we investigate the extent to which the kinetics of initiation of the component promoters of a genetic toggle switch affect its responsiveness to extrinsic noise, i.e., to cell-to-cell number variability in the components associated to gene expression dynamics.

To assess this we implement a stochastic model of a genetic toggle switch that accounts for cell-to-cell diversity in RNA polymerase numbers and whose parameter values are all taken from state-of-the-art microscopy measurements of single-cell RNAP, single-RNA, and single-cell protein numbers. We then execute stochastic simulations of model cells (Gillespie, 1977)(Lloyd-Price et al, 2012), each with a multi-step stochastic model of the genetic switch and whose RNAP numbers are, while constant in time, initially randomly drawn from a normal distribution.

To assess the relevance of the cell-to-cell variability in RNAP numbers as a function of the kinetics of initiation of the component promoters on the macro-scale dynamics of the switch, we perform simulations differing in the rate constants controlling these two variables.

Methods

Model of the Genetic Switch

We consider a dynamic model of the switch where transcription and translation allow RNA and protein production kinetics to differ widely in noise levels, depending on the rate constants. This model is the result of multiple studies, including genome-wide studies of the RNA numbers variability (Bernstein et al, 2002)(Taniguchi et al, 2010), of

Carole Knibbe et al, eds., Proceedings of the ECAL 2017, Lyon, France, 4-8 September 2017,
(Cambridge, MA: The MIT Press, ©2017 Massachusetts Institute of Technology).

the transcription dynamics of individual genes (Lloyd-Price et al, 2016), of the translation kinetics at the single protein level (Mitarai et al., 2008)(Bremer and Dennis, 1996)(Kennel, and Riezman, 1977), of protein folding and activation kinetics (Cormack et al, 1996), and of the structure of natural genetic switches (Neubauer and Calef, 1970)(Arkin et al, 1998).

Most importantly, all parameter values in the model are obtained from empirical data (Table 1). Note that, for simplicity, we assume a symmetric switch, with both genes having the same rate constant values.

Multi-step transcription initiation of an active promoter is modeled by Reactions (1), with i = 1,2, P_{ON}^{i} (Saecker et al, 2011). The closed complex (RP_c) is formed once a RNAP (R) binds to a free promoter (Chamberlin, 1974). Next, subsequent steps follow that form the open complex (RP_o^i) (Saecker et al, 2011)(Chamberlin, 1974). Finally, elongation starts (deHaseth et al, 1998), which clears the promoter and results in a produced RNA and the RNAP releasing. In (1), k_1 is the rate at which RNAPs find and bind to the promoter, k_2 is the open complex formation rate, k_3 is the promoter escape rate, and k_{-1} is the rate of reversibility of the closed complex.

Reactions (2) model the transitioning of promoter i to an inactive state (P_{OFF}^{i}) due to the binding/unbinding of a (active) repressor protein ($Prot^{j}_{folded}$), produced by gene j. Note that i, j = {1,2} with $i \neq j$:

$$P^{i}_{\mathrm{ON}} + R \underset{k_{-1}}{\overset{k_1}{\rightleftarrows}} RP^{i}_{c} \xrightarrow{k_2} RP^{i}_{o} \xrightarrow{k_3} R + P^{i}_{\mathrm{ON}} + \mathrm{rna}^{i} \quad (1)$$

$$P^{i}_{\mathrm{ON}} + \mathrm{Prot}^{j}_{folded} \underset{k_{ON}}{\overset{k_{OFF}}{\rightleftarrows}} P^{i}_{\mathrm{OFF}} \quad (2)$$

Reactions (3) and (4) model translation and subsequent protein folding and activation, respectively:

$$rna^{i} + Rib \xrightarrow{k_{rbs}} rna^{i} + Rib + \mathrm{Prot}^{i}_{unfolded} \quad (3)$$

$$\mathrm{Prot}^{i}_{unfolded} \xrightarrow{k_{fold}} \mathrm{Prot}^{i}_{folded} \quad (4)$$

Reactions (5) and (6) model degradation and dilution due to cell division of RNA and proteins, respectively:

$$rna^{i} \xrightarrow{kd_{RNA}} \varnothing \quad (5)$$

$$\mathrm{Prot}^{i}_{folded} \xrightarrow{kd_{P}} \varnothing \quad (6)$$

As the number of RNAPs differs between live sister cells of a genetically homogenous population (see e.g. (Bernstein et al, 2002)(Lloyd-Price et al, 2016)), in our model, in each cell the number of RNAPs is set to constant but is initially randomly generated from a normal distribution, N(x,y), where x and y are obtained from empirical data (Lloyd-Price et al, 2016). This is the source of extrinsic noise of the model cell population considered here and is the main innovation of our model when compared to previous stochastic models of gene expression that account for the delays caused by the closed and open complex formations (Lloyd-Price et al, 2016)(Roussel and Zhu, 2006)(Ribeiro et al, 2006).

Stochastic Simulations

We perform simulations using SGNS2 (Lloyd-Price et al, 2012), a simulator of chemical reaction systems whose dynamics is driven by the Stochastic Simulation Algorithm (Gillespie, 1977) that allows multi-time-delayed reactions (Roussel and Zhu, 2006) as well as hierarchical, interlinked compartments to be created, destroyed and divided at runtime, a feature used here to generate independent model cells.

Detection of Switches in the Dynamics of the Toggle Switch and Switching Frequency Quantification

To detect switches in the protein numbers over time (where a switch is a change in which protein is 'dominant'), at each time moment of the simulation, we calculate the difference between the numbers of $Prot_1$ and $Prot_2$.

To filter out of short, transient switches, we then make use a simple filter: if the absolute difference between the numbers of $Prot_1$ and $Prot_2$ is smaller than 100, we set the difference to 0. Finally, we count the total number of switches during the time series by obtaining the number of times the difference between the two protein numbers changes from positive to negative and from negative to positive.

Finally, we define the switching frequency (F) as:

$$F = \frac{n+1}{\Delta t} \quad (7)$$

where n is number of switches and Δt is observation time.

CV^2 of RNAP relative levels in individual cells

The empirical values of the RNAP numbers in individual cells were extracted from RNAP fluorescence intensity values in individual *E. coli* RL1314 cells with fluorescently tagged β' subunits (Lloyd-Price et al, 2016). From these, we set the mean RNAP fluorescence in individual cells arbitrarily to 1 and obtain the fraction of cells with a given relative fluorescence level. The 2.5% cells with lowest and highest fluorescence intensity are discarded as outliers. Next, we obtain the CV^2 of RNAP relative levels in individual cells by fitting a normal distribution to the data (MATLAB package *Statistics and Machine Learning Toolbox*™). The CV^2 of the fit equals 0.03, in agreement with (Lloyd-Price et al, 2016).

To validate the fitting, we performed a Kolmogorov-Smirnov (KS) test between the empirical and best fit distributions. It shows that they cannot be statistically distinguished (p-value of 0.69). We thus use the best fit distribution to set random RNAP numbers in each model cell.

Degradation and dilution of RNA and protein numbers due to cell divisions

We assume a mean cell lifetime (*div*) of 1 hour (Lloyd-Price et al, 2016). The dilution rate (*Dil*) of RNA and proteins thus equals:

$$Dil = div^{-1} \times \log(2) \quad (8)$$

Carole Knibbe et al, eds., Proceedings of the ECAL 2017, Lyon, France, 4-8 September 2017,
(Cambridge, MA: The MIT Press, ©2017 Massachusetts Institute of Technology).

Given the degradation rate (*Deg*), e.g. for RNA, the overall RNA decay rate (k_d) will be:

$$k_d = Dil + Deg \quad (9)$$

The same formula is applied to proteins, using the appropriate rate constant (kd_p) for the degradation process.

Parameter values and control model

Simulations use reactions (1)-(6) and the parameter values in Table 1 (unless stated otherwise). Simulations were initialized with only the two promoters of the switch (both in the ON state) (i.e. no proteins or RNAs). Figure 1 (left) illustrates the stochastic model switch and shows the resulting RNA (bottom right) and Protein numbers over time (top right) of an example simulation. Visibly, at the macroscale level, the circuit exhibits stochastic switching in protein and RNA numbers with a realistic time interval between switches (Neubauer and Calef, 1970).

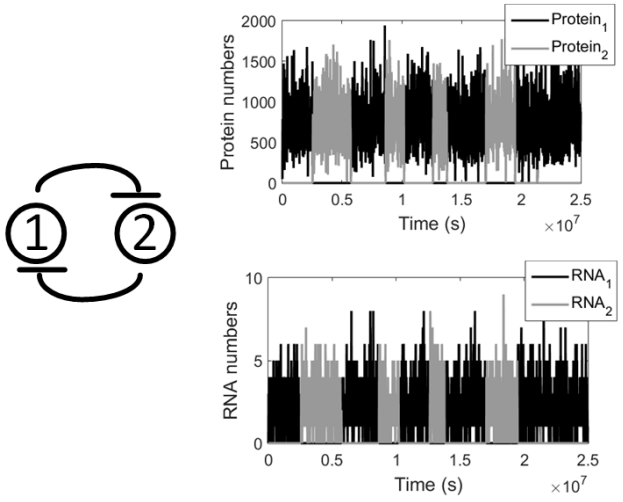

Figure 1: Illustrative image of a genetic toggle switch (left) and example time series of protein (top right) and RNA (bottom right) numbers from a stochastic simulation.

Parameter	Value (s^{-1})	Reference
k_{ON}	0.01	(Lloyd-Price et al, 2006)
k_{OFF}	281	(Lloyd-Price et al, 2006)
k_1	6469	(Lloyd-Price et al, 2006)
k_{-1}	1	(Lloyd-Price et al, 2006)
k_2	0.005	(Lloyd-Price et al, 2006)
k_3	∞	(Lloyd-Price et al, 2006)
kd_{rna}	0.002	(Bernstein et al, 2002), Eq. (8)
k_{rbs}	0.637	(Mitarai et al, 2008) (Bremer and Dennis, 1996) (Kennel and Riezman, 1977)
k_{fold}	0.0024	(Cormack et al, 1996)
kd_p	0.0019	(Cormack et al, 1996), Eq. (8)

Table 1: Parameter values of the model switch (control). k_1 and k_{rbs} values are set assuming that the number of available RNAP and Ribosomes equal 1 (but are never depleted).

We study the macro-scale kinetics of genetic switches (mean and cell the cell diversity in switching frequency) as a function of the cell-to-cell variability in RNAP numbers and of the kinetics of the closed and open complex formation (here controlled by tuning k_1 and k_2 respectively, (1)).

According to the model, e.g., increasing k_1 shortens the closed complex duration. Increasing k_2 shortens the open complex duration. We tuned k_1 and k_2 so that the mean RNA production rate is the same in all cases, using the following formula (Lloyd-Price et al, 2016):

$$I(R) = \frac{(k_{ON} + k_{OFF})(k_{-1} + k_2)}{Rk_1k_2k_{ON}} + \frac{1}{k_2} + \frac{1}{k_3} \quad (10)$$

Equation (10), derived from (1) and (2), defines I(R), the mean interval between consecutive RNA productions in individual cells, assuming infinite cell lifetime. In (10), we first set all parameter values to the controls values shown in Table 1, to obtain the value of I(R) in the control condition.

Next, we again use this formula, by setting all parameter values as in Table 1, except k_1 and k_2,, and setting I(R) to the value calculated using the control. From the resulting equation, we set k_1 to different values and calculate the corresponding value of k_2, to obtain models differing in k_1 and k_2, but having the same value for I(R) as the control model.

Note that, by changing k_1 and k_2, our goal is to change the mean time-length of the closed complex formation (τ_{cc}) relative to the mean interval between consecutive RNA production events (Δt). This fraction of time between consecutive RNA production events spent in closed complex formation ($\tau_{cc}/\Delta t$), is given by:

$$\frac{\tau_{cc}}{\Delta t} = \frac{(k_{ON} + k_{OFF})(k_{-1} + k_2)}{Rk_1k_2k_{ON}} \times I(R)^{-1} \quad (11)$$

Also, the range of values of k_1 and k_2 was set within realistic intervals (empirical values in Table 2 for various promoters and induction schemes (Kandavalli et al, 2016)).

Promoter and induction	$\tau_{cc}/\Delta t$
P_{BAD} (0.1% arabinose)	0.71
P_{BAD} (0.01% arabinose)	0.55
P_{BAD} (0.001% arabinose)	0.17
$P_{lac\text{-}O1O3}$ (1 mM IPTG)	0.55
$P_{lac\text{-}O1O3}$ (0.05 mM IPTG)	0.46
$P_{lac\text{-}O1O3}$ (0.005 mM IPTG)	0.12
P_{tetA} (no inducers)	0.07
$P_{lac\text{-}O1}$ (1 mM IPTG)	0.05
$P_{lac\text{-}ara1}$ (1 mM IPTG and 0.1% arabinose)	0.49

Table 2: Empirical values of $\tau_{cc}/\Delta t$ of various promoters subject to various induction levels.

Given this range of empirical values, we opted for simulating models that differ in $\tau_{cc}/\Delta t$ by +0.1, from 0.05 to 0.95 (i.e. 10 conditions). Meanwhile, for the RNAP cell-to-cell variability, the empirical data indicates a CV^2(RNAP) of 0.03. We opted for simulating models that differ in

Carole Knibbe et al, eds., Proceedings of the ECAL 2017, Lyon, France, 4-8 September 2017,
(Cambridge, MA: The MIT Press, ©2017 Massachusetts Institute of Technology).

CV^2(RNAP) by +0.015, from 0 to 0.09 (i.e. 7 conditions). Overall, we simulate 70 models.

Each model was simulated 100 independent times for $5x10^7$ seconds, with a sampling interval of 10^4 s.

Results and Conclusions

$\tau_{cc}/\Delta t$ acts as a tunable filter of cell-to-cell variability in RNAP numbers effects on the switch dynamics

We performed simulations for various values of $\tau_{cc}/\Delta t$ (controlled by changing k_1, k_2) and of the CV^2 of RNAP numbers (CV^2(RNAP)), including the control condition (Table 1). From the protein numbers over time, we first assessed the mean frequency of switching (*F*) (Methods) in each condition (Figure 2).

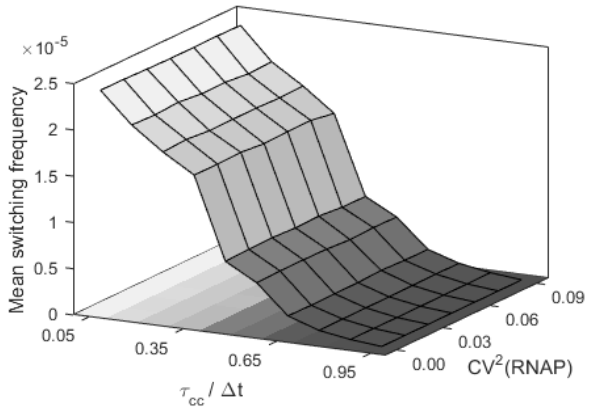

Figure 2: Mean switching frequency as a function of $\tau_{cc}/\Delta t$ and CV^2(RNAP). 100 independent cells per condition.

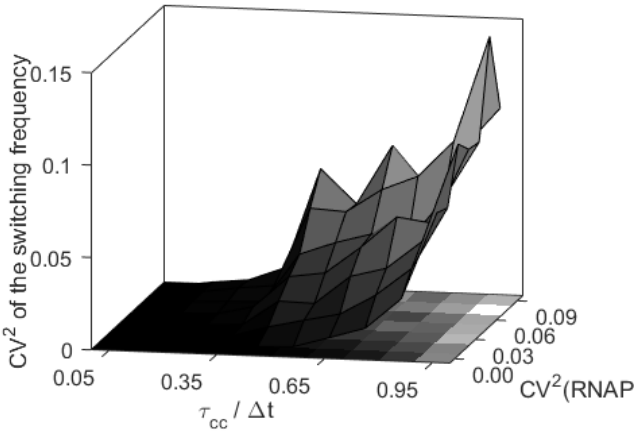

Figure 3: Cell-to-cell diversity (CV^2) of the switching frequency as a function of $\tau_{cc}/\Delta t$ and CV^2(RNAP). 100 independent cells per condition.

From Figure 2, the mean *F* is heavily affected by $\tau_{cc}/\Delta t$, Namely, increasing $\tau_{cc}/\Delta t$ stabilizes the 'noisy attractors' of the switch (Ribeiro and Kauffman, 2007c), since it reduces the chances of finding the promoter of the 'OFF' gene in a state that allows the RNAP to transcribe it.

Meanwhile, the mean F is not affected by the CV^2 in RNAP numbers. This is expected, as the CV^2(RNAP) of the cell population should not influence the mean behavior of the population, only its variability (as the variability in RNAP numbers is implemented by a symmetric normal distribution).

Next, Figure 3 shows that, as the CV^2(RNAP) increases, so does the CV^2 of the switching frequency of the cell population (provided that $\tau_{cc}/\Delta t$ is larger than ~0.35). Interestingly, $\tau_{cc}/\Delta t$ also plays a strong role in the cell-to-cell diversity in switching frequency, as the effects of extrinsic noise are filtered out from the dynamics of the genetic switches for small values of $\tau_{cc}/\Delta t$.

The CV^2(RNAP) only affects the CV^2(F) weakly for small values of $\tau_{cc}/\Delta t$ for two reasons. The main one is that the CV^2(RNAP) only affects the cell-to-cell variability of the mean duration of the closed complex formation. If this step is short-length, the effects on the overall variability in RNA production kinetics will be weak. Second, for relatively small values of $\tau_{cc}/\Delta t$ compared to $\tau_{oc}/\Delta t$, the dynamics of the switch is less stable (i.e. noisier) (Bahrudeen et al, 2017), causing the effects of increasing CV^2(RNAP) to become less visible.

Micro-scale dynamics of the switch is controlled by $\tau_{cc}/\Delta t$

Finally, we studied the extent to which $\tau_{cc}/\Delta t$ and CV^2(RNAP) control the cell to cell variability in protein numbers (micro-scale dynamics) of each individual gene integrated into a switch. As these numbers differ widely when the respective promoters are in 'ON' and 'OFF' states, we analyze them separately. Note that the cell to cell diversity in protein numbers is, in our context, equivalent to noise in protein numbers over time.

For this, from the simulations, for each condition, we collected both protein numbers in individual cells 1 million seconds after starting the simulation. Then, we determined which one was higher, and calculated the cell-to-cell variability (as measured by the CV^2) in protein numbers of the genes in 'ON' and 'OFF' states, separately. Results for genes in 'ON' state are shown in Figure 4 ($CV^2(Prot^{ON})$).

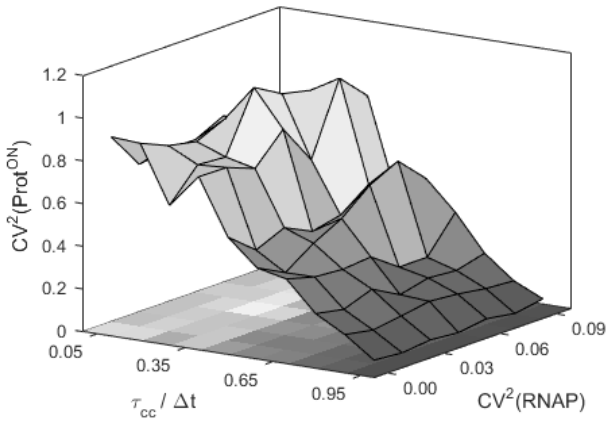

Figure 4: Cell-to-cell diversity in protein numbers in individual cells at a given point in time ($CV^2(Prot^{ON})$), as a function of $\tau_{cc}/\Delta t$ and CV^2(RNAP). 100 independent cells per condition.

Visibly, $\tau_{cc}/\Delta t$ can be used to regulate $CV^2(Prot^{ON})$: the higher is $\tau_{cc}/\Delta t$, the weaker is this quantity. Meanwhile,

Carole Knibbe et al, eds., Proceedings of the ECAL 2017, Lyon, France, 4-8 September 2017,
(Cambridge, MA: The MIT Press, ©2017 Massachusetts Institute of Technology).

CV^2(RNAP) does not affect $CV^2(Prot^{ON})$ significantly. This can be confirmed by calculating, from the 100 runs per condition, the Pearson correlation coefficient and respective p value between (CV^2(Proteins) and CV^2(RNAP). Results in Table 3 show that, in all cases, this correlation is not statistically significant (all p-values above 0.01).

$\tau_{cc}/\Delta t$	Pearson Correlation coefficient between $CV^2(Prot^{ON})$ and CV^2(RNAP)	p value
0.05	-0.553	0.198
0.15	-0.650	0.114
0.25	0.404	0.369
0.35	0.495	0.258
0.45	-0.066	0.888
0.55	0.830	0.021
0.65	-0.202	0.664
0.75	-0.087	0.853
0.85	-0.228	0.622
0.95	0.285	0.536

Table 3: Pearson correlation coefficient and p values between the (CV^2(Proteins) and the CV^2(RNAP) as a function of $\tau_{cc}/\Delta t$. The proteins considered are of the gene in the ON state.

Similarly, we found no correlation between CV^2(RNAP) and the $CV^2(Prot^{OFF})$ (Figure 5 and Table 4). Figure 5 further informs that, once more, the main regulator of the other component of the microscale dynamics of the switch (i.e. the protein numbers of the OFF gene), is $\tau_{cc}/\Delta t$.

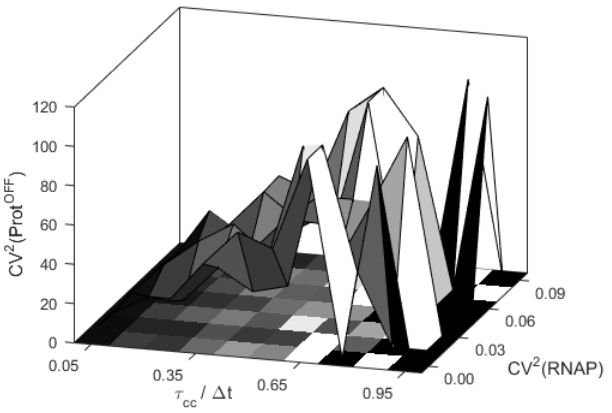

Figure 5: Cell-to-cell diversity in protein numbers ($CV^2(Prot^{OFF})$) in individual cells at a given point in time, as a function of $\tau_{cc}/\Delta t$ and CV^2(RNAP). 100 independent cells per condition.

We thus conclude that, under certain conditions the macroscale dynamics of the switch can be tuned by CV^2(RNAP). Meanwhile, the microscale dynamics is mostly determined solely by $\tau_{cc}/\Delta t$.

$\tau_{cc}/\Delta t$	Pearson Correlation coefficient between $CV^2(Prot^{OFF})$ and CV^2(RNAP)	p value
0.05	0.221	0.634
0.15	-0.188	0.686
0.25	-0.253	0.584
0.35	-0.243	0.600
0.45	-0.354	0.437
0.55	0.052	0.912
0.65	-0.439	0.325
0.75	0.032	0.945
0.85	-0.144	0.758
0.95	0.408	0.363

Table 4: Pearson correlation coefficient and p values between (CV^2(Proteins) and CV^2(RNAP) as a function of $\tau_{cc}/\Delta t$. The protein numbers considered are of the gene in the OFF state.

Discussion

We performed simulations of a stochastic model of a 2-gene toggle switch that includes the multi-step processes of transcription and translation and uses only experimentally validated parameter values (Lloyd-Price et al, 2006)(Bernstein et al, 2002)(Mitarai et al, 2008)(Bremer and Dennis, 1996)(Kennel and Riezman, 1977)(Cormack et al, 1996).

Interestingly, the behavior of the model switch (e.g. using the control rate constants ($\tau_{cc}/\Delta t$ = 0.81, CV^2(RNAP) = 0.03) is similar to that natural functional switches, with a mean switching frequency of ~ 52.6 days, i.e., 1262.4 cell lifetimes for a division rate of 1 hour (Neubauer and Calef, 1970).

Overall, we find that both the macrodynamics (switching frequency) and microdynamics (variability in protein numbers of both the ON and OFF gene) are more strongly regulated by $\tau_{cc}/\Delta t$ than by CV^2(RNAP). Importantly, in genes where the closed complex is short-length compared to the intervals between RNA productions, the effects of CV^2(RNAP) become almost negligible. In that sense, we conclude that the $\tau_{cc}/\Delta t$ of the component genes can act as filters of genetic circuits for extrinsic noise sources.

We found somewhat surprising that the cell-to-cell diversity in RNAP numbers has little to no effect on the cell-to-cell diversity in protein numbers. We believe that there are two reasons for this. First, it is likely due to the small empirical value of CV^2 (RNAP) (empirical value of ~0.03 and all values tested below 0.1). Second, and related to the first reason, it is likely due to the significant amount of other noise sources and their strength, most being intrinsic, such as the exponentially distributed duration of the open complex formation, which render negligible the contribution from RNAP numbers variability.

In the future, we plan to expand our research on how tuning the kinetics of initiation of the component genes may allow attaining desired levels of noise in the macrodynamics of various other genetic circuits, such as clocks and filters.

Carole Knibbe et al, eds., Proceedings of the ECAL 2017, Lyon, France, 4-8 September 2017,
(Cambridge, MA: The MIT Press, ©2017 Massachusetts Institute of Technology).

Acknowledgments

Work supported by Academy of Finland (proj. numbers 295027 to A.S.R and 305342 to A.S.R.), and Jane and Aatos Erkko Foundation (610536 to A.S.R.). The funders had no role in study design, data collection and analysis, decision to publish, or preparation of the manuscript.

References

Arkin, A., Ross, J., and McAdams, H. (1998) Stochastic Kinetic Analysis of Developmental Pathway Bifurcation in Phage λ-Infected Escherichia coli Cells. *Genetics* 149(4):1633-1648.

Bahrudeen, M.N.M., Startceva, S., and Ribeiro, A.S. (2017) Effects of extrinsic noise are promoter kinetics dependent. In Proceedings of the 9th International Conference on Bioinformatics and Biomedical Technology (ICBBT 2017), May 14-16, Lisbon, Portugal.

Bernstein, J.A., Khodursky, A.B., Pei-Hsun, L., Lin-Chao, S. and Cohen, S. N. (2002) Global analysis of mRNA decay and abundance in Escherichia coli at single-gene resolution using two-color fluorescent DNA microarrays. *Proc. Natl Acad. Sci*. USA 99:9697–9702.

Bremer, H. and Dennis, P.P. (1996) Modulation of Chemical Composition and Other Parameters of the Cell by Growth Rate. In: Neidhardt, F.C., (ed.), Escherichia Coli and Salmonella, 2nd ed. ASM Press, Washington, DC, 1553–1569.

Chamberlin, M.J. (1974) The selectivity of transcription, *Annu. Rev. Biochem.* 43:721–775.

Cormack, B.P., Valdivia, R.H., Falkow, S. (1996) FACS-optimized mutants of the green fluorescent protein (GFP). *Gene* 173(1):33-38.

deHaseth, P.L., Zupancic, M.L. and Record, M.T. (1998) RNA polymerasepromoter interactions: The comings and goings of RNA polymerase. *J. Bacteriol.* 180:3019–3025.

Farewell, A., Kvint, K., Nyström, T. (1998) Negative regulation by RpoS: A case of sigma factor competition, *Mol. Microbiol*. 29:1039–1051.

Gillespie, D.T. (1977) Exact stochastic simulation of coupled chemical reactions. J. Phys. Chem. 81(25):2340–2361.

Hengge-Aronis, R. (2002) Recent insights into the general stress response regulatory network in Escherichia coli. J. *Mol. Microbiol. Biotechnol.* 4 :341–346.

Jishage, M., Iwata, A., Ueda, S., Ishihama, A. (1996) Regulation of RNA polymerase sigma sub-unit synthesis in Escherichia coli: intracellular levels of four species of sigma subunit under various growth conditions. *J. Bacteriol.* 178:5447–5451.

Kandavalli, V.K., Tran, H. and Ribeiro, A.S. (2016) Effects of σ factor competition on the in vivo kinetics of transcription initiation in Escherichia coli. BBA Gene Regulatory Mechanisms 1859:1281–1288.

Kennel, D., and Riezman, H. (1977) Transcription and translation initiation frequencies of the *Escherichia coli* lac operon. *J. Mol. Biol.* 114(1):1-21.

Lloyd-Price, J., Startceva, S., Kandavalli, V., Chandraseelan, J., Goncalves, N., Oliveira, S.M.D., Häkkinen, A. and Ribeiro, A.S. (2016) Dissecting the stochastic transcription initiation process in live Escherichia coli. *DNA Research* 23(3):203-214.

Lloyd-Price, J., Gupta, A, and Ribeiro, A.S. (2012) SGNS2: A Compartmentalized Stochastic Chemical Kinetics Simulator for Dynamic Cell Populations. *Bioinformatics* 28:3004-3005.

MATLAB and Statistics and Machine Learning Toolbox Release 2016b, The MathWorks, Inc., Natick, Massachusetts, United States. In Press Publication.

McClure, W.R. (1980) Rate-limiting steps in RNA chain initiation. *Proc. Natl Acad. Sci. USA* 77:5634–5648.

Mitarai, N., Sneppen, K., Pedersen, S. (2008) Ribosome collisions and translation efficiency: optimization by codon usage and mRNA destabilization. *J. Mol. Biol.* 382(1):236-245.

Neubauer, Z., and Calef, E., (1970) Immunity Phase-shift in Defective Lysogens: Non-mutational Hereditary Change of Early Regulation of λ Prophage. *J. Mol. Biol.* 51:1-13.

Rahman, M., Hasan, M.R., Oba, T. , Shimizu, K. (2006) Effect of rpoS gene knockout on the metabolism of Escherichia coli during exponential growth phase and early stationary phase based on gene expressions, enzyme activities and intracellular metabolite concentrations. *Biotechnol. Bioeng*. 94:585–595.

Ribeiro, A.S., Zhu, R. and Kauffman, S.A. (2006) A General Modeling Strategy for Gene Regulatory Networks with Stochastic Dynamics. *J. of Comput. Biol.* 13:1630-1639.

Ribeiro, A.S. (2007a) Effects of coupling strength and space on the dynamics of coupled toggle switches in stochastic gene networks with multiple-delayed reactions, *Phys. Rev. E* 75(6):061903. DOI: 10.1103/PhysRevE.75.061903.

Ribeiro, A.S. (2007b) Dynamics of a two-dimensional model of cell tissues with coupled stochastic gene networks, *Phys. Rev. E* 76(5):051915. DOI: 10.1103/PhysRevE.76.051915.

Ribeiro, A.S., and Kauffman, S.A., (2007c) Noisy Attractors and Ergodic Sets in Models of Gene Regulatory Networks, *J. of Theor. Biol.* 247(4):743-755. DOI: 10.1016/j.jtbi.2007.04.020.

Roussel, M.R. and Zhu, R. (2006) Validation of an algorithm for delay stochastic simulation of transcription and translation in prokaryotic gene expression. *Phys Biol.* 3(4):274-284.

Saecker, R.M., Record, M.T. and Dehaseth, P.L. (2011) Mechanism of bacterial transcription initiation: RNA polymerase - promoter binding, isomerization to initiation-competent open complexes, and initiation of RNA synthesis. *J. Mol. Biol.* 412:754–771.

Taniguchi, Y., Choi, P.J., Li, G.-W., et al. (2010) Quantifying E. coli proteome and transcriptome with single-molecule sensitivity in single cells. *Science* 329:533–538.

Carole Knibbe et al, eds., Proceedings of the ECAL 2017, Lyon, France, 4-8 September 2017,
(Cambridge, MA: The MIT Press, ©2017 Massachusetts Institute of Technology).